Acta Crystallographica Section D
Biological Crystallography
ISSN 0907-4449

The effect of protein–precipitant interfaces and applied shear on the nucleation and growth of lysozyme crystals

Nuno M. Reis,[a] Dimitri Y. Chirgadze,[b] Tom L. Blundell[b] and Malcolm R. Mackley[a]*

[a]Department of Chemical Engineering and Biotechnology, University of Cambridge, Pembroke Street, Cambridge CB2 3RA, England, and [b]Department of Biochemistry, University of Cambridge, 80 Tennis Court Road, Cambridge CB2 1GA, England

Correspondence e-mail: mrm5@cam.ac.uk

Received 6 April 2009
Accepted 10 August 2009

This paper is concerned with the effect of protein–precipitant interfaces and externally applied shear on the nucleation and growth kinetics of hen egg-white lysozyme crystals. The early stages of microbatch crystallization of lysozyme were explored using both optical and confocal fluorescence microscopy imaging. Initially, an antisolvent (precipitant) was added to a protein drop and the optical development of the protein–precipitant interface was followed with time. In the presence of the water-soluble polymer poly(ethylene glycol) (PEG) a sharp interface was observed to form immediately within the drop, giving an initial clear separation between the lighter protein solution and the heavier precipitant. This interface subsequently became unstable and quickly developed within a few seconds into several unstable 'fingers' that represented regions of high concentration-gradient interfaces. Confocal microscopy demonstrated that the subsequent nucleation of protein crystals occurred preferentially in the region of these interfaces. Additional experiments using an optical shearing system demonstrated that oscillatory shear significantly decreased nucleation rates whilst extending the growth period of the lysozyme crystals. The experimental observations relating to both nucleation and growth have relevance in developing efficient and reliable protocols for general crystallization procedures and the controlled crystallization of single large high-quality protein crystals for use in X-ray crystallography.

1. Introduction

The degree of supersaturation of a protein solution and the rate at which such supersaturation is generated are generally major parameters that influence a crystallization process and control both nucleation and growth (Wiencek, 1999). If high supersaturation is reached rapidly, many crystals are nucleated (Luft *et al.*, 1994; García-Ruiz, 2003); consequently, antisolvent addition is often used for batch crystallization of high-value-added pharmaceutical products in order to control the nucleation kinetics (Charmolue & Rousseau, 1991). The experimental protocols used for the production of specialist single-crystal protein crystals for high-resolution X-ray diffraction studies continue to rely on the individual skill of the protein crystallographer and often wide empirical screening studies have to be covered before suitable conditions are found for the growth of a small number of crystals that are sufficiently large to be used for X-ray diffraction (Kam *et al.*, 1978; Wiencek, 1999).

The presence of concentration gradients is known to affect crystal growth and they can form during crystallization as protein-depletion regions around growing crystals (Kam *et al.*, 1978). However, to date the role of protein–precipitant inter-

faces during protein crystallization has not been examined in any detail. In addition, the use of external shear to enhance convection and the quality of protein crystals has not been investigated in relation to protein-crystal formation. Thus, a key aspect of this paper is to explore both the effect of composition interfaces and oscillatory shear on the nucleation and growth of a model protein crystal.

The crystallization process of proteins can be divided into three stages: (i) nucleation, (ii) post-nucleation growth and (iii) cessation of growth (Feher & Kam, 1985; Fitzgerald & Madsen, 1986). The importance of the nucleation stage has been emphasized by García-Ruiz (2003) and it is clear that the nucleation step can control both the structure of the crystallizing phase and the number and the size of the crystals produced. The time required for the formation of a nucleus depends strongly on the 'height' of the nucleation barrier $\Delta G_{\rm nuc}$ and thus on the level of supersaturation (Durbin & Feher, 1996). The number of nuclei N forming per unit of time t (known as the nucleation rate; $B \equiv {\rm d}N/{\rm d}t$) depends not only on the free-energy barrier but also on the supersaturation and the volume of the system (García-Ruiz, 2003), with direct implications in the scale-up of crystallization conditions from 'nanodrops' to 'microdrops' (Bodenstaff *et al.*, 2002).

The growth rate of crystals is determined by the rate of transport (diffusion or convection) of protein molecules to the crystal surface and the probability of attachment of a molecule (thus becoming incorporated in the surface of the crystal). Small crystallization volumes tend to suppress convection, as does growth in gels or in solutions in which the viscosity has been increased by the addition of synthetic polymers or glycerol. Convection effects are also minimized by crystallization in microgravity, although variations in the surface tension can drive convection in this case (Rosenberger, 1986).

In the absence of convection, the protein molecules are transported through the solution by diffusion. A concentration gradient necessarily develops and the solution nearer the crystal is relatively depleted of protein. This has the important consequence that nucleation is inhibited in the vicinity of a growing crystal. In the extreme case of diffusion-limited growth, the protein concentration at the crystal surface $C_{\rm s}$ drops to the solubility limit C^* (the concentration at equilibrium). Under these conditions, the linear growth rate G (*i.e.* the average speed of advance of the exposed crystallographic faces) is given by (Durbin & Feher, 1996)

$$G \equiv {\rm d}L/{\rm d}t = D(C_{\rm b} - C_{\rm s})V/\delta, \qquad (1)$$

where D is the diffusion coefficient, V is the volume occupied by a molecule in the crystal and δ is the boundary layer; that is, the effective distance over which a molecule must diffuse to go from the bulk solution at concentration $C_{\rm b}$ to the crystal surface at concentration $C_{\rm s}$. When diffusion is the only transport mechanism, δ is of the order of the crystal radius; larger crystals must attract molecules from farther away. Thus, the diffusion-limited growth rate decreases with time as the crystal grows. In the case of lysozyme, the diffusion coefficient D (1.59×10^{-10} m^2 s^{-1}) was found to be that of the protein monomer (Feher & Kam, 1985; Kam *et al.*, 1978; Miyashita *et al.*, 1994).

Crystals naturally cease to grow as the protein concentration drops to the solubility limit C^*. However, it has been observed that growth may cease even at higher concentrations and not restart unless the supersaturation is very high. This phenomenon has mostly been studied with lysozyme (Durbin & Feher, 1996; Feher & Kam, 1985; Kam *et al.*, 1978). Hypotheses advanced to explain such cessation include the random accumulation of lattice defects as the crystal grows (Feher & Kam, 1985) and the adsorption of impurities or denatured protein molecules (Durbin & Feher, 1986; Durbin *et al.*, 1993).

It is believed that the incorporation of defects on the surface of protein crystals is also associated with the mass-transport regime of protein molecules from the solution to the surface of the crystals. Attempts to crystallize proteins in a microgravity environment in spacecraft (*i.e.* with reduced convection) have thus far been inconclusive; however, the use of external mixing as a means of enhancing the transport of protein molecules should equally result in an enhancement of crystal quality as suggested by the regime transport model presented by Rosenberger (1986). Nevertheless, the well known fragility of protein crystals (Wiencek, 1999) limits attempts of crystallographers to use high-shear environments in protein crystallization.

The routine use of robotic systems for automated crystallization trials is based on the assumption that mixing happens 'spontaneously' in a crystallization drop as a consequence of the simple coalescence of protein drop and precipitant agent (Bard *et al.*, 2004; D'Arcy *et al.*, 2004; Chayen *et al.*, 1990). Surveys on automatic systems for protein crystallization have been presented, for example by D'Arcy *et al.* (2004), Bard *et al.* (2004) and Stevens (2000). In a standard microbatch crystallization experiment, mixing within the drop actually relies on molecular diffusion and therefore mixing times are not necessarily short when compared with the timescale for aggregation (Durbin & Feher, 1996). Such irreproducible passive mixing in crystallization drops could be the major factor responsible for uncertainties in batch protein crystallization (Chen *et al.*, 2004).

Protein crystallization from solution also has certain similarities to the way synthetic polymers crystallize from supercooled solutions and Keller (1968) eloquently described how polyethylene chains crystallize to form chain lamella single crystals. It was also discovered that flow had a profound effect on the way polyethylene crystallized, as not only were the nucleation and growth kinetics affected by flow but the morphology of the resulting crystals could also be very different (Keller, 1968; Mackley & Keller, 1975). The use of flow shear during different stages of protein crystallization has not been explored in detail, although some recent theories, simulations and studies (Penikova *et al.*, 2006 and references therein) have recently shown that shear flow can actually have an important effect in the nucleation of crystals from solution. Penikova *et al.* (2006) have demonstrated the strong effect of shear in the range 10^{-3}–10^{-1} s^{-1} on crystal nucleation. The use of a peri-

odic oscillatory flow in the vicinity of a growing face seems to reduce the 'interface instabilities' at the surface of the growing crystals, resulting in higher quality crystals when compared with crystals grown in either stagnant or laminar flow (Chew *et al.*, 2004). This was demonstrated by Chew *et al.* (2004) by showing that paracetamol crystals with enhanced surface characteristics were produced in an oscillatory baffled batch crystallizer in comparison with those obtained in an impeller-driven batch crystallizer.

Recent developments in the area of microfluidics now offer the possibility of running nanolitre-scale trials of protein crystallization in a microenvironment in the presence of controlled shear flow (Chen *et al.*, 2005; Shim *et al.*, 2007). There is now a strong belief that the protein-nucleation process is sensitive to flow rate and mixing (Chen *et al.*, 2005).

The effects of concentration gradients and protein–precipitant interfaces in the early stages of protein crystallization remain neglected. The existence of concentration gradients and a protein–precipitant interface in the crystallization drop can influence both nucleation and crystal growth by presenting regions of enhanced supersaturation and extended nucleation. A combination of optical and confocal imaging visualization techniques are described in this paper, establishing the effect of concentration gradients and protein–precipitant interfaces during the microbatch crystallization of the model protein hen egg-white lysozyme. In addition, shear has been applied in a systematic and controlled way to explore the effect that this has on both nucleation and growth.

2. Experimental procedures

2.1. Materials

Lysozyme from chicken egg white (molecular weight $\simeq$ 14 600 Da) was used as a test protein. Dialysed sixfold lyophilized lysozyme (EC 3.2.1.17; $\sim$100 000 units mg^{-1}) produced by Fluka was obtained from Sigma–Aldrich (Gillingham, England). Poly(ethylene glycol) monomethyl ether solution with an average relative molecular weight of 5000 (PEG 5000 MME, CAS 9004-74-4) and a weight concentration of 50% in water was used and light mineral oil (CAS 804-47-5; average density of 0.862 at 298 K) were also obtained from Sigma and were of molecular-biology grade. Anhydrous sodium acetate (CAS 127-09-3) and sodium chloride (CAS 7647-14-5) of analytical grade were also obtained from Sigma. Fluoroscein isothiocyanate (FITC 'Isomer I') and Alexa Fluor 633 C5 maleimide (relative molecular weight $\simeq$ 1300 Da) used in the confocal imaging studies were supplied by Invitrogen (Paisley, Scotland).

2.2. Crystallization experiments

All crystallization experiments were performed at room temperature (about 293 K) using the microbatch-under-oil procedure (Chayen *et al.*, 1990; Table 1). Protein solutions were prepared by dissolving a certain mass of lysozyme in 1 ml Milli-Q ultrapure water in an Eppendorf tube to achieve a final concentration of 100 mg ml^{-1}. Care was taken to not use high shear during the dissolution of the protein. The protein solution was then ultracentrifuged for 5 min at 10 000 rev min^{-1} and the supernatant was collected and used in the crystallization trials.

Table 1
Properties of the liquid solutions used in the crystallization trials.

Fluid	Specific mass (g ml^{-1})	Viscosity (kg m^{-1} s^{-1})
Protein solution	1.022	1.26
Precipitant	1.091	22.75
Mineral oil	0.862	24.72

Aqueous drops of protein and precipitant [30%(*w*/*v*) PEG 5000 MME, 1 *M* NaCl, 50 m*M* sodium acetate buffer pH 4.5] were combined in a 1:1 ratio under a thick layer of light mineral oil in order to minimize evaporation. Controls were carried out in a V-bottom Sero-Wel 96-well microbatch plate (Bibby Sterilin Ltd, Staffordshire, England) by filling the microwell with 100 µl mineral oil and pipetting 2 µl protein solution followed by 2 µl precipitant agent (Fig. 1*a*). Microwell plates were then covered and incubated; care was taken to not exert any vigorous movement during the manipulation of the plates.

2.3. Confocal fluorescence imaging experiments

Lysozyme was labelled with FITC by dissolving 10 mg lysozyme in 1 ml 0.1 *M* carbonate/bicarbonate buffer pH 8.3 and mixing it with 0.5 ml of a solution of 1 mg ml^{-1} FITC in dimethyl sulfoxide. The mixture was then wrapped in aluminium foil and incubated for 1 h on a rotary shaker at low speed at room temperature. The free dye was separated from the labelled protein using a disposable PD-10 desalting gel-filtration column (GE Healthcare, Buckinghamshire, England) pre-packed with Sephadex G-25 medium. The column was first equilibrated with 20 ml ultrapure water and then loaded with 1 ml reaction mixture and eluted with a series of 1 ml ultrapure water. 1 ml fractions were collected and the eluted labelled protein was collected in the first 700 µl of fraction 5.

For crystallization trials in the confocal imaging microscope, a glass-bottom culture dish (Mattek Corporation, Ashland, Massachusetts, USA) was filled with a thick layer of mineral oil and thereafter fitted in the wide-stage of a Leica TCS SP5 confocal imaging microscope (Leica Microsystems, Milton Keynes, England). Unlabelled lysozyme solution (100 mg ml^{-1}) was then mixed with a small portion of labelled protein in a 10:1 ratio and 0.5–2 µl was dispensed with a micropipette into the centre of the culture dish, followed by the same volume of precipitant (Fig. 1*b*). Optionally, the precipitant solution was 'labelled' with an aqueous solution of Alexa Fluor 633 (a fluorophor with a far-red emission) in a 1:100 ratio, giving a final concentration of Alexa Fluor 633 of about 100 µg ml^{-1} in the precipitant. The crystallization drop was then scanned with a 10× magnification lens and 20 stacks were acquired at different heights of the drop in time intervals of $\sim$10 s. The maximum volume of the drop scanned was $\sim$1 × 1 × 1 mm.

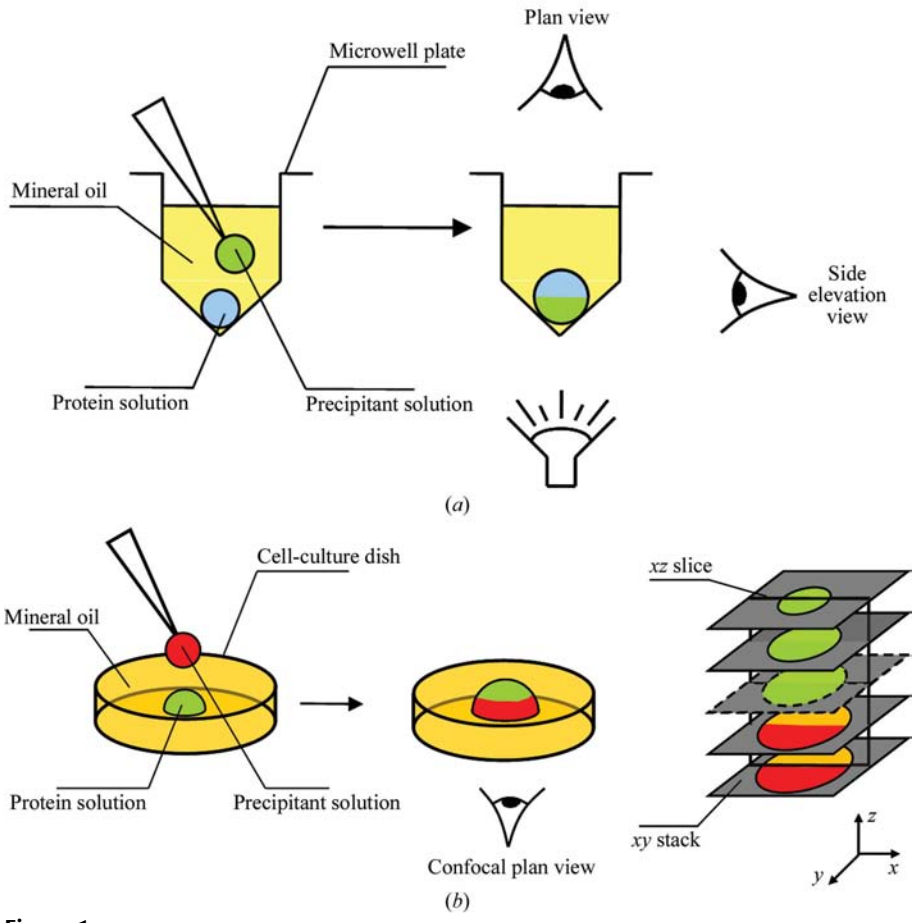

Figure 1
Schematic procedures and viewing planes used for microscopic analysis of microbatch crystallization of lysozyme using (*a*) optical imaging and (*b*) confocal fluorescence imaging.

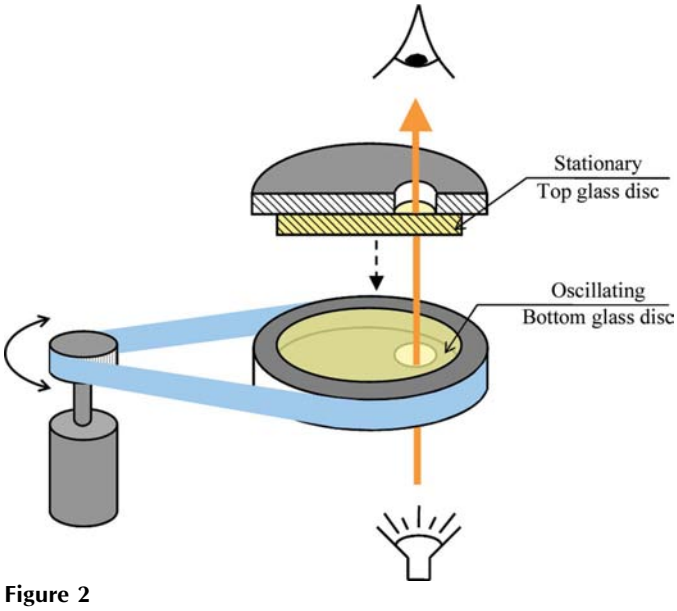

Figure 2
Schematic of the Linkam Cambridge Shear Cell System used for studying the effect of shear on the crystallization of lysozyme. The protein drop and precipitant were dispensed into the centre of the observation point within the reservoir in the bottom plate, which is located 7.5 mm out the centre of rotation.

FITC was excited at a wavelength of 488 nm and Alexa Fluor at 633 nm, giving two distinct emission spectra for the labelled protein and precipitant solutions. Images of the fluorescence were recorded in different channels in addition to the brightfield image of the drop. The image-analysis software *ImageJ* (developed at the National Institute of Mental Health, Maryland, USA) was then used to generate two-dimensional and three-dimensional projections of the fluorescence level as well as vertical plots (*i.e.* re-slices) of the fluorescence level in the drops at different *xz* planes (Fig. 1*b*).

2.4. Oscillatory shear experiments

Fig. 2 shows a simplified schematic of the Linkam Cambridge Shear System used for studying the effect of shear in the crystallization of lysozyme. This shear system, which was invented by the Polymer Fluids Group at the University of Cambridge (Mackley *et al.*, 1999), allows the study of flow microstructure and crystallization processes in the presence of different shear modes, such as steady and oscillatory shear. It basically consists of two quartz pieces independently attached to a removable top plate and a fixed bottom plate. The quartz piece in the bottom plate has a holding volume for the sample and can be rotated by a stepper motor controlled *via* a PC. This movement induces a linear gradient of velocities in the sample along the *z* direction (thus a homogenous shear field). The gap size between the two plates can be accurately adjusted in the range 0–2500 µm by a set of four pins also controlled *via* a PC by a second stepper motor (not illustrated). The bottom plate can also be harmonically oscillated given a frequency and maximum strain amplitude. An Olympus CCD camera attached to the shear system allows the visualization and recording (plan view) of the sample throughout the shearing process.

Crystallizations in the shear system were carried out by filling the sample volume in the bottom plate with 2 ml light mineral oil and dispensing 2 µl protein solution into the centre of the visualization field (a point eccentric to the centre of rotation, as shown in Fig. 1) followed by 2 µl precipitant. The top plate was then attached and the shearing started simultaneously with the video recording. An oscillatory shear mode was chosen as it allows the observation of a set of crystals throughout the crystallization time, therefore enabling the evaluation of the crystal-growth kinetics. The gap size used in this work was 1.0 mm and a shear strain of 5% at a frequency of 1 s^{-1} was selected, giving a maximum periodic shear rate of

$\sim$47 s^{-1}. The intensity of the light source was minimized throughout the experiment in order to avoid sample overheating.

3. Results and discussion

Chicken egg-white lysozyme was used as a model protein as it is highly soluble in water and produces crystals in a short time. Following the addition of precipitant, the first crystals were typically visible within 2 min when working with 100 mg ml^{-1} lysozyme in the protein solution. This provided a convenient time scale for both the confocal imaging microscope and shear-system experiments.

Fig. 3 summarizes the plan view of the first 2 h of lysozyme crystallization in a V-bottom 96-well microbatch plate. An intense 'optical' convection was observed immediately after merging of the heavier precipitant and the lighter protein drops in the microwell which lasted at least 4–5 min. A larger number of tetragonal crystals quickly developed in the crystallization drop and continued to grow for approximately 2 h, when the crystals reached a terminal size of $\sim$100 µm. The first crystals were detected after 2–3 min with a 4× magnification lens. As the crystals grew, a second stage of intensive convection marked by the intensive transport of small particles (either protein or salt) was observed, which was presumably related to the high concentration gradients in the drop.

A more detailed analysis of the first 2 min of recording in the microbatch crystallization of lysozyme revealed the development of an unsteady interface between the protein and precipitant, which resembles inter-penetrating fingering instabilities reported by Rayleigh (1882) and G. I. Taylor (1950). Furthermore, the location of the first visible crystals (within the first 60 s of the experiment) seemed to correlate with the interface of these fingering regions.

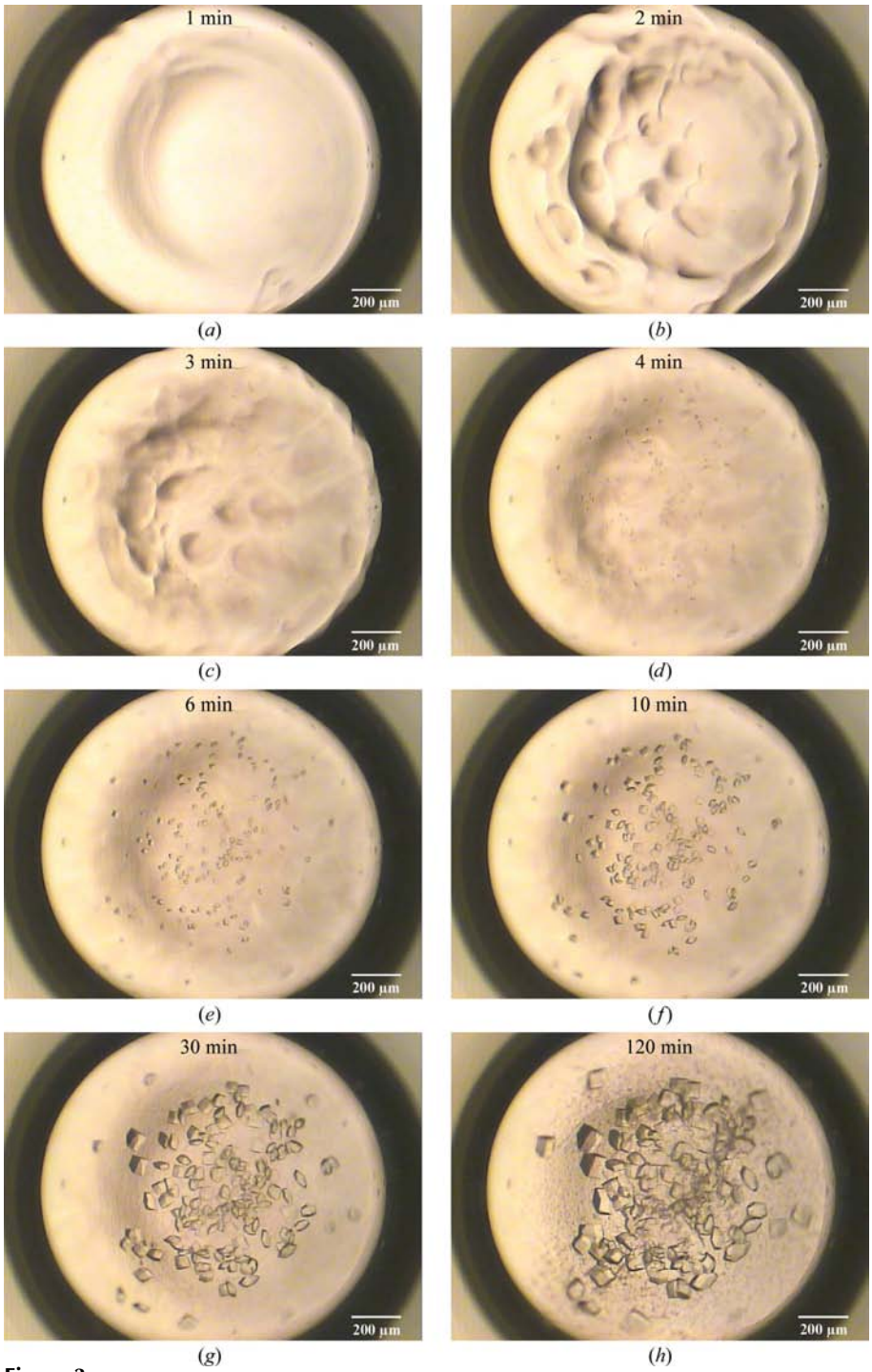

Figure 3
Top plan view of microbatch crystallization of 2 µl lysozyme solution (100 mg ml^{-1}) with 2 µl precipitant [30%(*w*/*v*) PEG 5000 MME, 1 *M* NaCl, 50 m*M* sodium acetate buffer pH 4.5] in a V-bottom 96-well microbatch plate.

3.1. Optical imaging of interface development

The plan-view recording of the early interface-mixing process revealed strong convection accompanying the microbatch crystallization process of lysozyme; nevertheless, an improved insight could be obtained by examining the vertical concentration distribution in the crystallization drops from a side-elevation view and with confocal microscopy. Therefore, similar experiments were carried out in a 96-well microbatch plate and the mixing process in the crystallization drop was recorded from a side elevation for the early stages of the crystallization. A small amount of

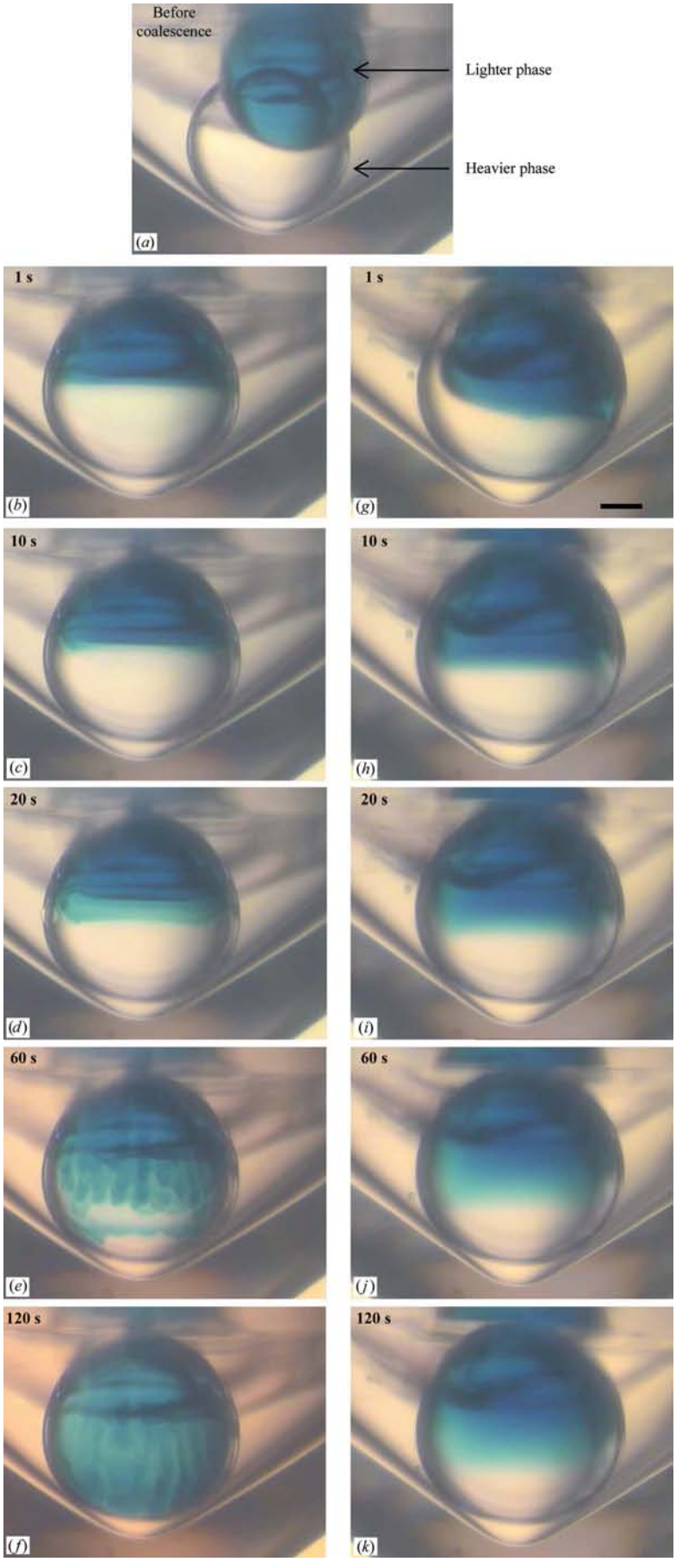

blue food dye was added to the lighter solution (protein) to help to enhance the visualization of the protein–precipitant mixing in the merged drop. This was further compared with the mixing process in a drop with no protein present. The microbatch plate was immersed in glycerol to minimize the optical effects through the outer cylindrical walls of the microwells; a light diffuser assured a homogeneous white background. Fig. 4 summarizes the migration of the blue dye from the lighter phase to the precipitant solution (*i.e.* the heavier phase) in the first 2 min following the coalescence of the two aqueous drops.

A major observation in Fig. 4 is the immediate formation of a sharp interface separating the heavier precipitant (with a density of 1.091) and the lighter protein solution (with a density of 1.022) from the merging of the two aqueous drops. The interface was sharper after ∼1.3 s [sequence (*b*)–(*f*) in Fig. 4] and was equally visible for the experiment in the absence of protein in the lighter solution [sequence (*g*)–(*k*) in Fig. 4]. The blue dye in the lighter phase thereafter showed a progression towards the bottom of the drop by means of molecular diffusion and/or mass convection. A major difference between the two runs shown in Fig. 4 was the 'stepwise' progression of the dye in the protein–precipitant drop, which can be identified by the 'steps' in colour intensity in the dye interface. This was then followed by the development of a characteristic 'fingering' of the interface after ∼27 s.

Another significant difference between the two experiments shown in Fig. 4 is the higher velocity of migration of the dye interface in the protein–precipitant drop in comparison with the migration of the same dye in the water–precipitant drop. In the latter, the dye dispersion occurs by simple molecular diffusion. The dispersion coefficient for the food dye, $D_{\rm dye}$, in the water–precipitant drop can be estimated from the images as of the order of $1 \times 10^{-9}\ {\rm m^2\ s^{-1}}$ using Einstein's correlation, $x = (2D_{\rm dye} \times t)^{1/2}$, where x is the displacement in the time interval t. The typical value of $D_{\rm LM}$ reported for the lysozyme monomer ($D_{\rm LM} = 1.12 \times 10^{-10}\ {\rm m^2\ s^{-1}}$; Judge *et al.*, 1999) is about one order of

Figure 4
Side-elevation view of the mixing and coalescence of aqueous drops in a V-bottom 96-well microbatch plate under mineral oil. (*a*) shows the two drops instants before coalescing. The sequence (*b*)–(*f*) refers to 2 µl lysozyme solution (100 mg ml^{-1}) labelled with blue food dye followed by 2 µl precipitant. The sequence (*g*)–(*k*) refers to the mixing of 2 µl ultrapure water labelled with blue food dye with 2 µl precipitant. In both cases the precipitant used was 30%(*w*/*v*) PEG 5000 MME, 1 *M* NaCl, 50 m*M* sodium acetate buffer pH 4.5.

magnitude lower than that of D_{dye}; therefore, it can be concluded that the observed fingering process is associated with a sudden increase in the density of the protein such as protein precipitation.

The presence of the salt in the precipitant causes the protein to come 'out' as a separate solid phase *via* a 'salting-out' process (Arakawa & Timasheff, 1985) and induces an additional attraction between protein molecules known as the Hofmeister effect (Tardieu *et al.*, 2002). On the other hand, the water-soluble polymer PEG 5000 MME present in the precipitant induces a exclusion-volume effect on the protein (Middaugh *et al.*, 1979): the protein is sterically excluded from regions of the solvent occupied by the polymer, thus being concentrated until its solubility is exceeded and precipitation occurs, as the density of lysozyme crystals is 1.23 g cm^{-3} (Atha & Ingham, 1981).

3.2. Confocal fluorescence imaging of interface development

The fluorescence labelling of lysozyme allowed a greater insight into the development of protein concentration gradients in the crystallization drop with a confocal fluorescence microscope. For this purpose, experiments were carried out using the same microbatch-under-oil procedure but now with a flat-bottomed glass culture dish as this gives a maximum quality of scanned images. The hydrophilic surface of the culture dish represented a different contact angle of the drop with the surface in comparison with the contact angle in the hydrophobic plastic microwell plates (*i.e.* 180°). Therefore, the crystallization drops in these experiments assumed a flattened spheroid shape.

A series of 20 confocal image stacks were taken at a regular time interval (about 10 s), allowing the quantification of the fluorescence level at different positions along the z direction locations of the drop. Lysozyme solution at a concentration of 100 mg ml^{-1} was dyed with an FITC-labelled lysozyme solution (concentration ∼10 mg ml^{-1}) in a 10:1 ratio. This provided a protein solution with a diluted fluorescent dye and a good signal-to-noise ratio for the scanning.

Fig. 5 shows the z projection of protein fluorescence in a 2 µl drop following addition of the precipitant solution (only the protein solution was labelled in these experiments). The immediate formation of an interface between the lighter protein and heavier precipitant was confirmed, which quickly developed into a large fingering interfacial area containing regions with very high protein concentration gradients. After 50–60 s the 'fingering' regions containing protein at high concentration reached the flattened bottom of the drop, forming a layer with intense fluorescence in the bottom of the culture dish. The onset of nucleation was detected in the fluorescence images after 2 min and continued throughout the entire experiment (maximum time of 10 min). Brightfield

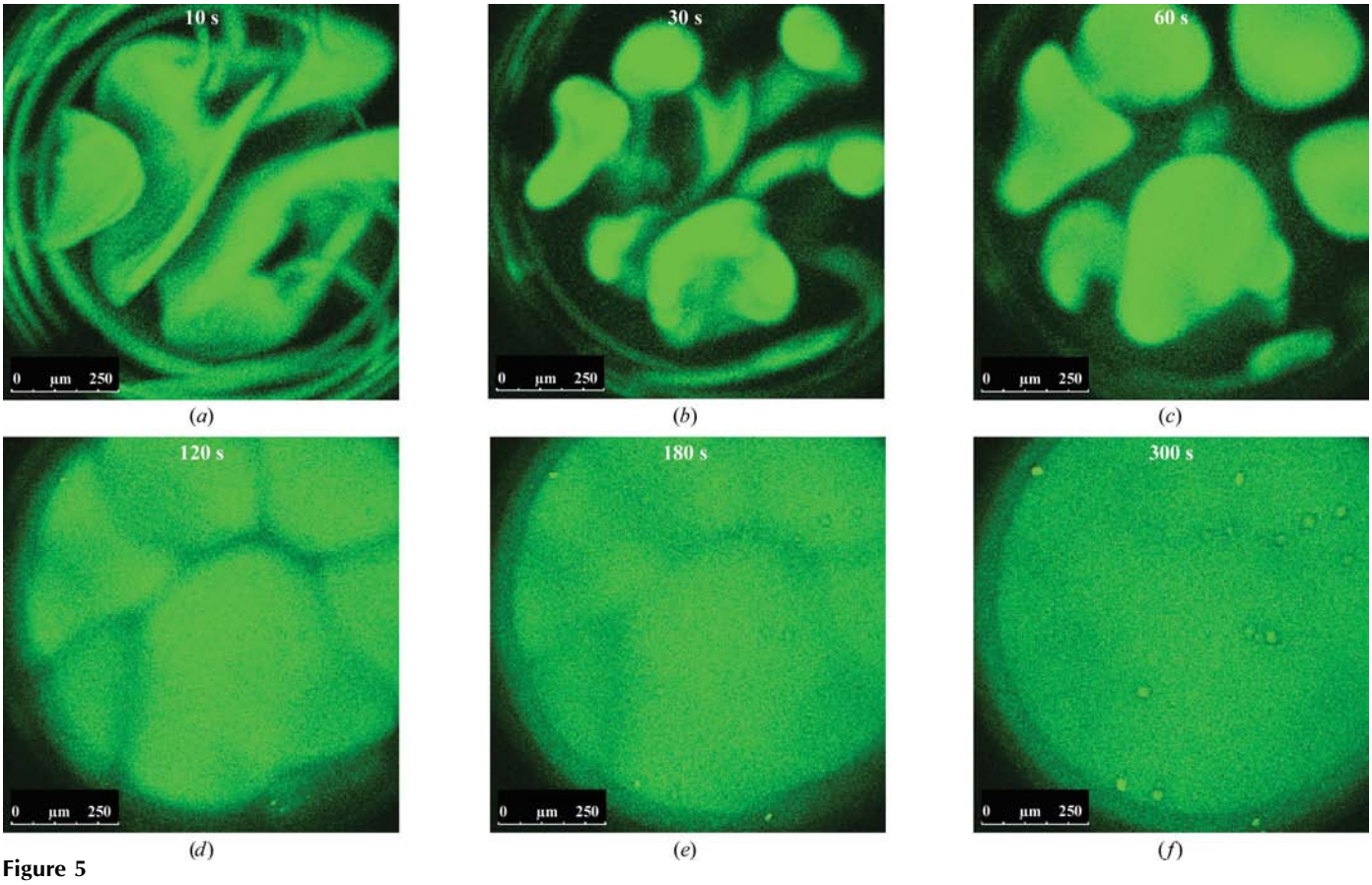

Figure 5
z projection of peak lysozyme fluorescence in microbatch crystallization of lysozyme in a glass tissue cell culture, showing the time development of instabilities in a 2 µl volume crystallization drop (*i.e.* 1 µl protein solution + 1 µl precipitant).

images, which give a better contrast between the crystals and the mother solution, allowed the detection of the first lysozyme crystals after 50–60 s of crystallization and a considerable number of crystals formed during the following 20–30 s.

The timescale of protein migration agrees well with the side-elevation view using the blue dye, especially when taking into consideration the fact that the flattened drop in the confocal image presents a lower migration path for the protein. The fluorescent images confirmed that the fingering process is associated with the precipitation and settling of protein.

The onset of crystals as detected in the brightfield images could be correlated with the interfacial regions in the fluorescence images. Crystal nucleation was concluded to occur preferentially at the interfacial regions having high protein concentration. This is exemplified in Fig. 6, where the set of onset crystals was manually tracked as they became visible. The position of the crystals correlated well with the location of the interfaces for each time frame. This was somehow expected as such interfacial regions present high concentration gradients of protein and precipitation and therefore increased the supersaturation and enhanced nucleation rates. This is the first time that such an effect has been experimentally demonstrated during the crystallization of a protein.

The experiments with confocal fluorescence imaging have also clearly shown that the large number of lysozyme crystals is a natural outcome of the high supersaturation and the large protein–precipitant interfacial area generated in the crystallization drop. This agrees with the conclusions of Chen *et al.* (2005) for the crystallization of another model protein (thaumatin) that the nucleation rate in microbatch crystallization is affected by the area and lifetime of the interface.

The Rayleigh–Taylor instability relies on a higher density of the liquid in the top phase supported by a lighter fluid in the bottom phase (Rayleigh, 1883; Taylor, 1950). In the crystallization experiments described in this paper, the density of the top phase is initially lower than the density of the bottom phase (precipitant). This is illustrated in Fig. 7, where the evolution of vertical *xz* profiles at a central plane of a crystallization drop is presented. It would appear that after the interface has formed, transport of components across the interface results in the development of higher local density in the top phase (protein) and the potential to become unstable. Note that the plots present a remarkable symmetry related to

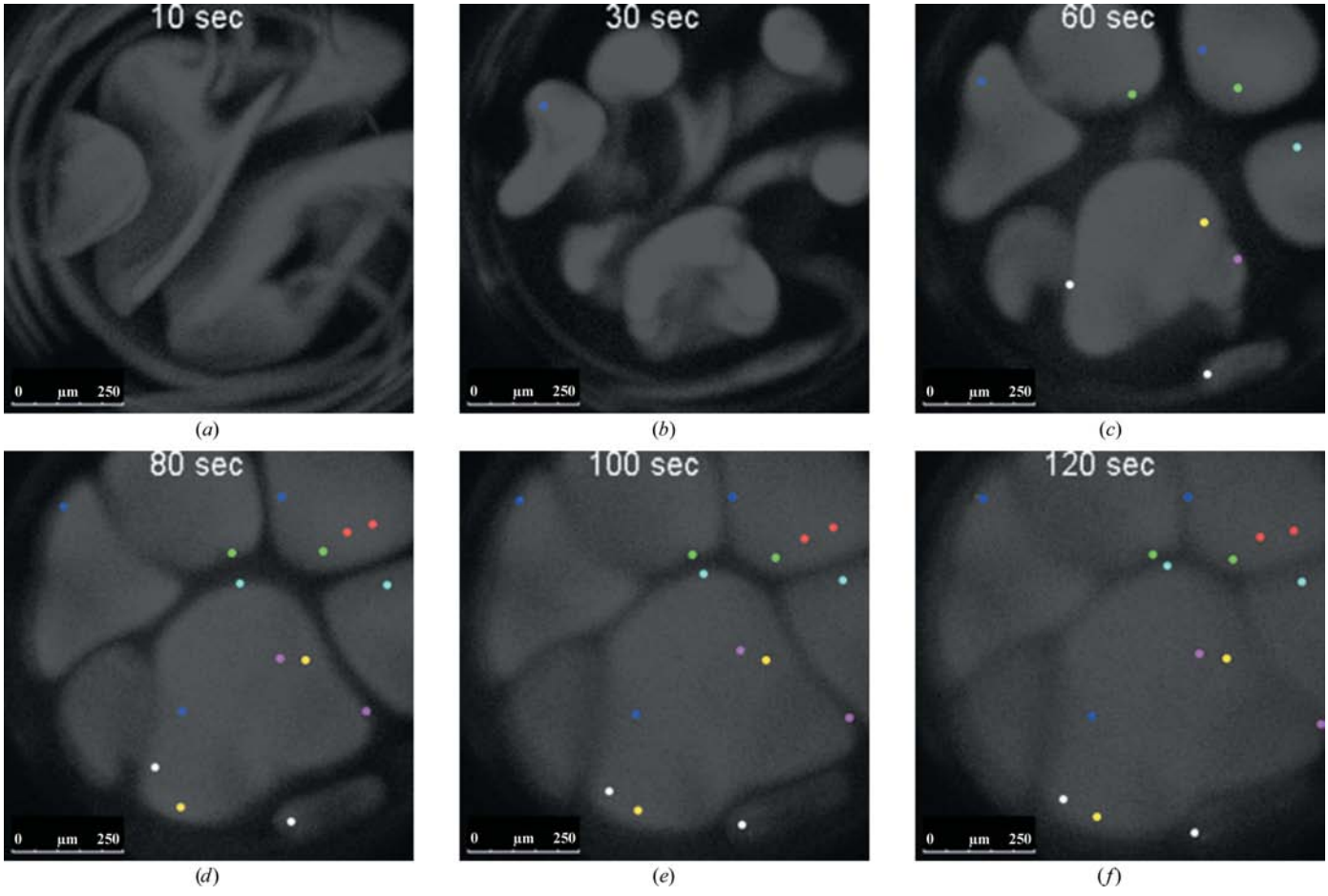

Figure 6
Manual tracking of the onset of lysozyme crystals in a 2 µl microbatch crystallization drop (the same experiment as presented in Fig. 5). The coloured dots in the foreground represent the position of each lysozyme crystal as visible in the brightfield image (data not shown), whilst the respective greyscale image of the *z* projection of peak protein fluorescence is shown in the background.

the smaller size of the drop; 0.5 µl FITC-labelled protein solution was combined with 0.5 µl Alexa 633-dyed precipitant solution, giving a 1 µl crystallization drop.

3.3. The effect of shear on lysozyme crystallization

Fig. 8 shows a sequence of lysozyme crystals grown in the Linkam Cambridge Shear System during a 48 h period. The application of oscillatory shear had a significant effect on the number and size of crystals formed. In the absence of shear, the experiments within the shear system and within the microwell plate gave a similar number and terminal size of crystals (~100 µm). The application of a low oscillatory shear at a frequency of 1 s^{-1} resulted in the production of fewer but larger lysozyme crystals (Fig. 8*b*). Oscillatory shear significantly reduced the nucleation rate.

The experiments in the Linkam Cambridge Shear System were performed with a time lag in shearing at the beginning of

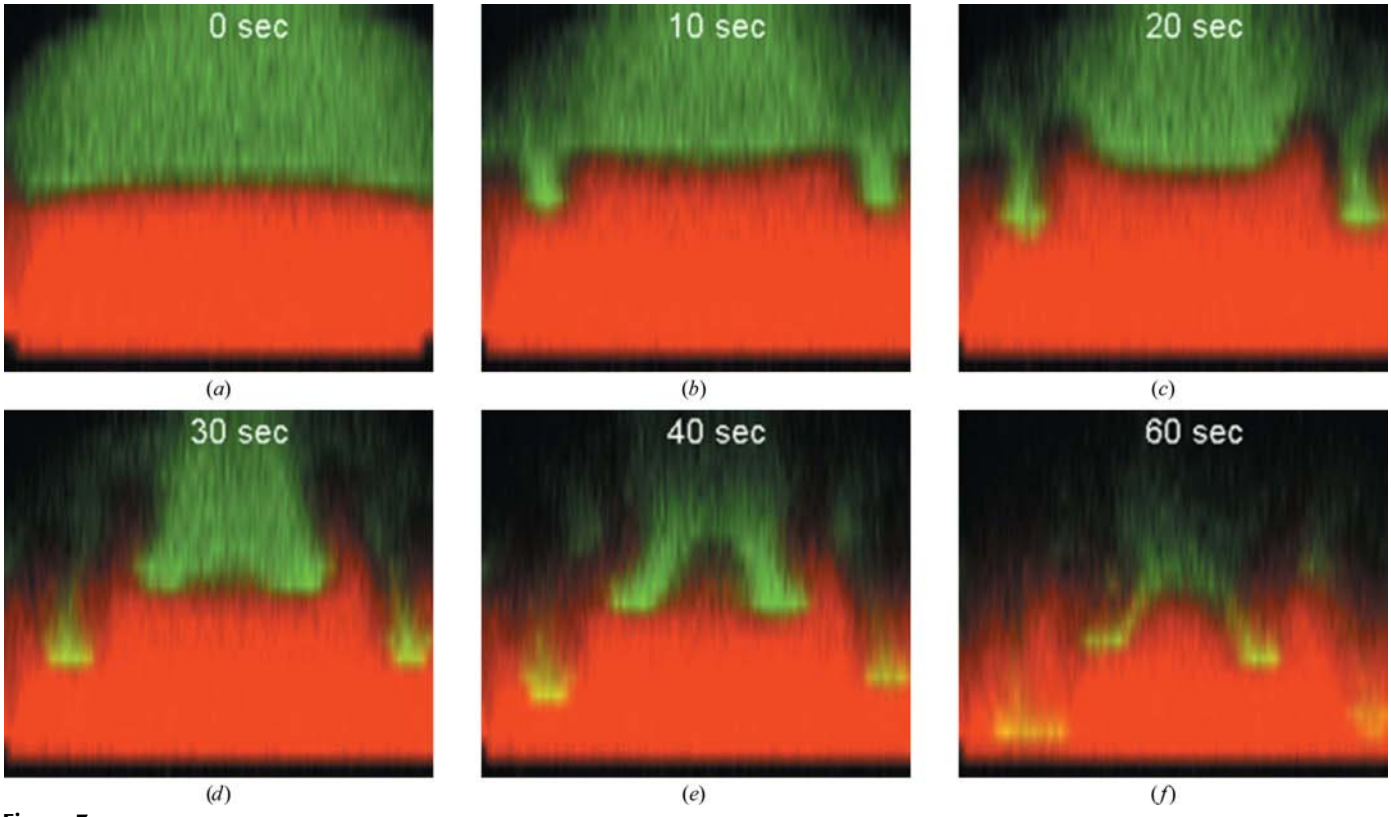

Figure 7
Time evolution of *xz* fluorescence of FTIC (green colour; labelled lysozyme) and Alexa 633 (red colour; dissolved in the precipitant) in the centre of a 1 µl crystallization drop (0.5 µl FITC-labelled lysozyme solution + 0.5 µl Alexa 633-dyed precipitant). These vertical plots were obtained by re-slicing and interpolating each of the 20 *xy* stacks as illustrated in Fig. 1(*b*).

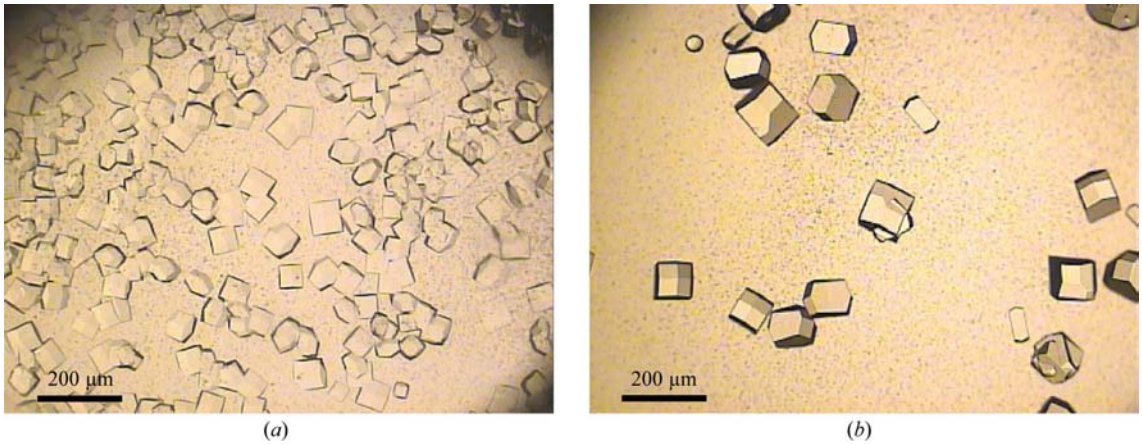

Figure 8
Lysozyme crystals grown for 48 h using the microbatch-under-oil method in the Linkam Cambridge Shear System. (*a*) No shear, 1 mm gap. (*b*) Oscillatory shear 1 s^{-1}, shear rate 47 s^{-1}, 1 mm gap size. Crystallization conditions: 2 µl lysozyme solution (100 mg ml^{-1}) combined with 2 µl precipitant [30%(*w*/*v*) PEG 5000 MME, 1 *M* NaCl, 50 m*M* sodium acetate buffer pH 4.5].

the experiments. The top plate had to be assembled after the protein and precipitant drops had been dispensed into the holding volume of the bottom plate. In the experiment shown in Fig. 8(*b*) shear was started within the first minute of crystallization. By the start of the video recording, the fingering interfaces (resembling a wave formation in the plan view of the optical microscope) had already developed. With the start of shearing most of these 'waves' quickly dissipated and a lower number of crystals emerged from the solution. Shear had the ability to accelerate interfacial mass mixing and thus minimize the concentration gradients in the drop and decrease local regions of high supersaturation lifetime. Chen *et al.* (2005) have drawn similar conclusions from their work on thaumatin crystallization with microcapillaries at increasing flow rates. They found that the number of protein crystals in crystallization microdroplets decreased with increasing flow rate for an incubation time of 3 h at 291 K and therefore

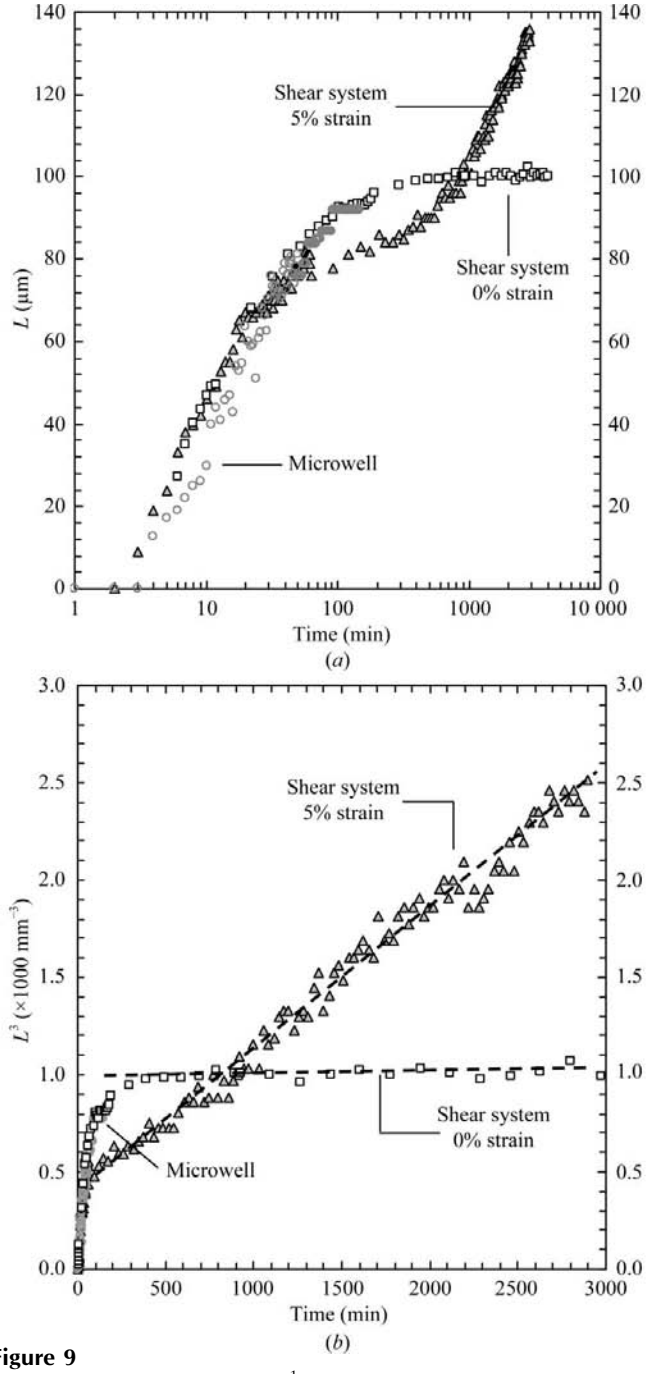

Figure 9
Effect of oscillatory shear (1 s^{-1}, 1 mm gap size, 5% strain, shear rate 47 s^{-1}) in the microbatch crystallization of lysozyme. (*a*) Crystal size (*L*). (*b*) Crystal volume (L^3). The rate of volume increase in the presence of oscillatory shear after 50 min is ~0.72 mm^3 min^{-1}, R^2 = 0.992.

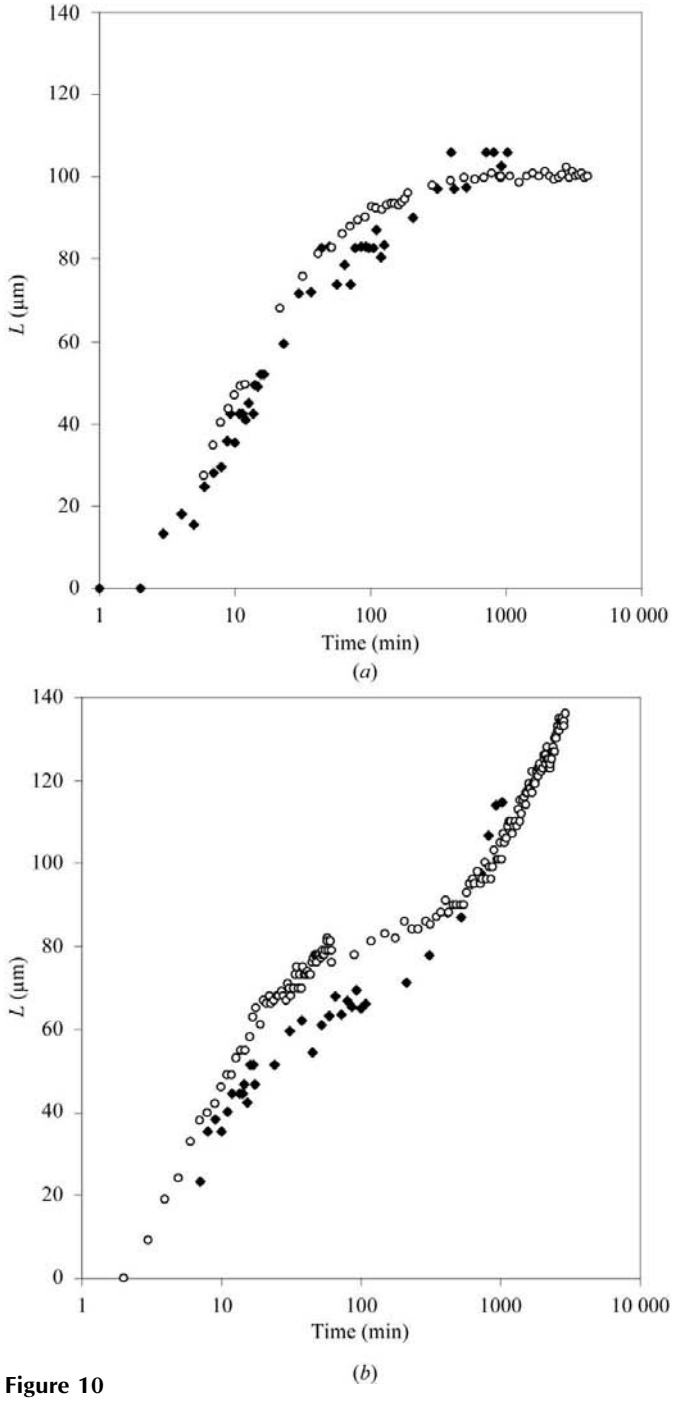

Figure 10
Reproducibility of microbatch crystallization of lysozyme in the Linkam Cambridge Shear System. (*a*) No shear, 1 mm gap size. (*b*) Oscillatory shear, 1 s^{-1}, 1 mm gap size, 5% strain, shear rate 47 s^{-1}. Each data series shows a different crystal randomly selected from experimental duplicates.

concluded that the nucleation rate in microbatch crystallization was affected by the area and the lifetime of the interface between the solutions rather than simply by the mixing time.

The time evolution of crystal size, L, for a randomly selected crystal during the first 48 h is plotted in Fig. 9, which highlights further differences in growth kinetics in the presence of oscillatory shear. Independently of the shear of the microenvironment, the lysozyme crystals showed a constant growth rate during the initial 10 min of incubation, as seen in Fig. 9(*a*). The values determined for the linear growth rate, G, were between 3.5 µm min^{-1} (for the experiment in the static microwell) and 5.3 µm min^{-1} (for the experiment with oscillatory shear in the shear system). These values of G are of the same order of magnitude as those published by Durbin & Feher (1986) for lysozyme. During this initial time interval, the crystal growth is limited by the attachment rate.

After this initial time of constant growth and in the absence of shear, G quickly decreases and crystals cease growing and reach a terminal size of ∼100 µm before 500 min. With the growth of crystals the protein is quickly consumed from the solution and therefore G becomes diffusion-limited. A further plausible explanation is the accumulation of defects on the surface of the crystals (Feher & Kam, 1985) rather than the simple depletion of precipitated protein, as a second stage of growth was observed between 80 and 150 h of incubation (data not shown), which resulted in a further 10% increase in L.

The kinetics of crystal growth for the diffusion-limited stage significantly differed with the introduction of oscillatory shear (Fig. 9*b*). In these conditions of enhanced mass transport, lysozyme crystals continued to grow for longer and reached a 30–40% larger terminal size (*i.e.* $L \simeq 140$ µm) after 48 h. The plot of L^3 *versus* time in Fig. 9(*b*) shows a constant rate of deposition of protein mass in the surface of the crystal after the initial 50 min of the experiment (a constant increase in the crystal volume of ∼0.72 mm^3 min^{-1}). The use of gentle shearing in protein crystallization enhances the transport of protein molecules and probably allows the removal of impurities or defects that would otherwise be accumulating naturally on the surface of the crystals and would prematurely end crystal growth. The parameter L^3 in Fig. 9(*b*) was selected as being representative of the volume and mass of the crystals.

Fig. 10 shows a time plot of L for different crystals in experimental duplicates which illustrates the data reproducibility (an important parameter in protein crystallization).

The set of experiments in the Linkam shear cell system have shown the possibility of improving mass transport and enhancing the overall crystal growth without breaking the weak ionic interactions and hydrogen bonds in the protein crystals.

3.4. The importance of solution interfaces in the control of crystal nucleation

Crystallization of lysozyme in the presence of PEG 5000 MME and salt is unusual as nucleation readily occurs within a few minutes and for the conditions described here nucleation was readily visible within the first minute. In order to produce few large crystals for X-ray studies, the uncontrolled nucleation generated by the local interface concentration gradients at the beginning of the crystallization trial is neither required nor desirable. If, however, other protein systems are used which are very much more difficult to nucleate it may well be that the introduction of such interfaces can be used for strategic benefit to induce or enhance nucleation at the early stages.

An understanding of the conditions under which microbatch crystallization occurs through the combination of a protein solution C_A with a precipitant (antisolvent) C_B can be gained from Fig. 11. Assuming that mixing occurs spontaneously (case 1; a common assumption in automated crystallization trials), mixing of C_A and C_B leads to a crystallization drop with homogeneous concentrations of protein and precipitant equal to $C_A/2$ and $C_B/2$, respectively. In this scenario, the supersaturation in the crystallization drop is low and probably not sufficient to trigger the onset of crystal formation. For some other situations, especially those involving the use of water-soluble synthetic polymers such as PEG (case 2), the combination of C_A and C_B would result in the formation of a clear sharp interface in the crystallization drop. The driving force for nucleation (*i.e.* supersaturation) in this interface is clearly enhanced, therefore resulting in the formation of a larger number of crystals. The supersaturation in the crystallization drop can then gradually be moved towards point 1 by means of forced mixing (*i.e.* convection) or molecular diffusion. However, the development of 'fingering instabilities' associated with the use of water-soluble polymers as demonstrated in this paper for lysozyme would induce the formation of a large interfacial area between the protein and the precipitant, encouraging the onset of a large number of crystals.

Case 1 in Fig. 11 corresponds to a situation in which the nucleation rate is well controlled and homogenous in the entire volume of the drop, where the crystals formed would presumably present the best desirable quality. Nevertheless, the overall low supersaturation in the crystallization drop as seen in the phase diagram would limit the possibility of

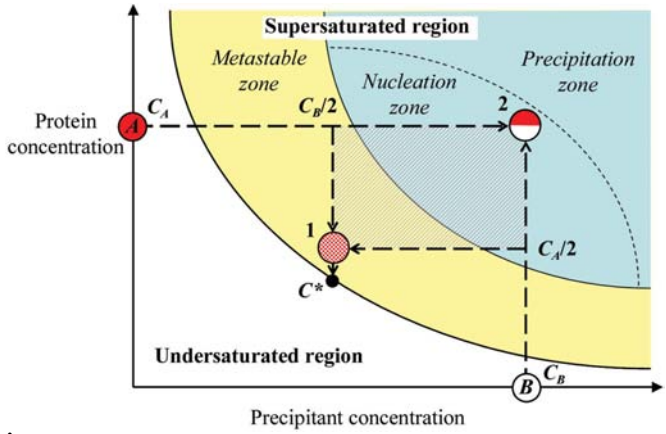

Figure 11
Possible crystallization pathways in a microbatch crystallization in the presence of solution interfaces.

nucleation taking place. The microbatch crystallization trials would return no visible crystals unless nucleation was triggered by an interface or impurity. This is particularly important for solutions of protein presenting low solubility or for crystallization trials in nanolitre drops as the nucleation rate is directly proportional to the volume of the drop. Under such conditions, the formation of a sharp interface as shown for case 2 (at least for a defined time interval, to be fine-tuned according to the protein involved) might be advantageous for shortening the total time required for nucleation (often the limiting step in protein crystallization) as well as to produce the required supersaturation for the onset of crystals. This is also relevant to vapour-diffusion experiments as the sharp interface may allow a confined space for enhanced nucleation.

For protein crystallizations involving the use of a water-soluble polymer in the precipitant the mixing time might be significant in relation to the nucleation time, therefore every crystallization drop would present volume regions with distinct levels of supersaturation that can fit into any region of the phase diagram defined by the dashed area in Fig. 11. This probably explains uncertainties in batch protein crystallization in the absence of forced external mixing, as mentioned previously (Chen *et al.*, 2004).

A major difficulty associated with using a sharp interface to enhance the nucleation rate is the consequent development of further 'fingering' regions with high concentration gradients from that interface, leading to some extent to uncontrolled nucleation events. The formation of such 'fingering instabilities' is undesirable when the final goal is the formation of a single large crystal, as is the case for X-ray diffraction studies. We are currently exploring protocols to stabilize the sharp interface. The experiments with lysozyme in the shear system have shown that flow shear is a possible strategy. Chen *et al.* (2005) also suggested using rapid chaotic mixing to control precipitation or excessive nucleation at high supersaturation (pushing the solution towards point 1 in Fig. 11), whereas a gentle mixing (allowing the development of a microenvironment closer to point 2 in Fig. 11) would induce the necessary nucleation to a low-supersaturated solution.

4. Conclusions

In this work, we have reported a set of observations related to the control of crystal nucleation and growth in microbatch crystallization using lysozyme. The formation of an initial protein–precipitant interface in the crystallization drop can result in the development of fingering instabilities with enhanced supersaturation ratios, which in turn promote the spontaneous onset of nucleation and subsequent growth of protein crystals. The presence of a water-soluble synthetic polymer in the precipitant (PEG 5000 MME) induced the development of a large protein–precipitant interfacial area within the crystallization drop, representing regions with high concentration gradients of protein and precipitant and thereby providing a local range of different supersaturation conditions.

The above findings are relevant for the interpretation of screened protein crystallization conditions. In some cases the interface development between a precipitant solution (only containing salt) and a protein solution is very fast (of the order of a few seconds) and thus the mixing time is short compared with the timescale for crystallization. However, in other cases the interface develops into fingering instabilities on a timescale of 200–300 s as supported by both optical and confocal fluorescence microscopy imaging recording. The fingering instabilities resemble Rayleigh–Taylor instabilities in appearance and are presumably driven by density differences between the two solutions. The exact mechanism of the fingering instability is not known at present, but it is certainly linked to density, concentration differences and competing interfacial diffusion of species across the interface.

In a further set of experiments, the advantage of applying oscillatory shear during the crystallization of proteins was demonstrated. The use of oscillatory shear at a frequency of $1\ s^{-1}$ produced a maximum shear rate of the order of $47\ s^{-1}$ and caused a significant reduction in nucleation and significantly enhanced the overall crystal-growth kinetics. A mechanism that would explain both reduced nucleation and enhanced growth is at present not clear. The shearing action can be expected to aid in the homogenization of local concentration gradients and to assist transport to a crystal surface; however, the kinetics of both events are complicated and occur on both nano and meso length scales.

These new findings should help in developing improved general protocols for growing single large protein crystals to be used, for example, in X-ray studies and also in producing controlled nucleation and growth conditions for smaller crystals.

The formation of an initial sharp protein–precipitant interface in a crystallizing drop is of potential value as it can accelerate the nucleation stage, which is generally a limiting step in protein crystallization. Once a nucleus has formed, the protein–precipitant interface should quickly be dissipated, eventually by the action of an applied controlled shear. Crystal growth would then be favoured in the homogenous microenvironment.

The authors are grateful to Alexander Edwards for help setting up the confocal fluorescence imaging and to Ping Lao from HKUST for motivating discussions. NR and DC would like to thank the European Commission (Intra-European Marie Curie Fellowship programme) and the Wellcome Trust, respectively, for providing financial support.

References

Arakawa, T. & Timasheff, S. N. (1985). *Methods Enzymol.* **114**, 49–77.
Atha, D. & Ingham, K. (1981). *J. Biol. Chem.* **256**, 12108–12117.
Bard, J., Ercolani, K., Svenson, K., Olland, A. & Somers, W. (2004). *Methods*, **34**, 329–347.
Bodenstaff, E. R., Hoedemaeker, F. J., Kuil, M. E., de Vrind, H. P. M. & Abrahams, J. P. (2002). *Acta Cryst.* D**58**, 1901–1906.
Charmolue, H. & Rousseau, R. W. (1991). *AIChE J.* **37**, 1121–1128.
Chayen, N. E., Shaw Stewart, P. D., Maeder, D. L. & Blow, D. M. (1990). *J. Appl. Cryst.* **23**, 297–302.
Chen, D. L., Gerdts, C. J. & Ismagilov, R. F. (2005). *J. Am. Chem. Soc.* **127**, 9672–9673.

Chen, P. C., Chen, C. C., Fun, M. H., Liao, O. Y., Jiang, J. J., Wang, Y. S. & Chen, C. S. (2004). *Chem. Eng. Technol.* **27**, 519–528.
Chew, C. M., Ristic, R. I., Dennehy, R. D. & De Yoreo, J. J. (2004). *Cryst. Growth Des.* **4**, 1045–1052.
D'Arcy, A., Mac Sweeney, A. & Haber, A. (2004). *Methods*, **34**, 323–328.
Durbin, S. D., Carlson, W. E. & Saros, M. T. (1993). *J. Phys. D Appl. Phys.* **26**, B128–B132.
Durbin, S. D. & Feher, G. (1986). *J. Cryst. Growth*, **76**, 583–592.
Durbin, S. D. & Feher, G. (1996). *Annu. Rev. Phys. Chem.* **47**, 171–204.
Feher, G. & Kam, Z. (1985). *Methods Enzymol.* **114**, 77–112.
Fitzgerald, P. M. D. & Madsen, N. B. (1986). *J. Cryst. Growth*, **76**, 600–606.
García-Ruiz, J. M. (2003). *J. Struct. Biol.* **142**, 22–31.
Judge, R. A., Jacobs, R. S., Frazier, T., Snell, E. H. & Pusey, M. L. (1999). *Biophys. J.* **77**, 1585–1593.
Kam, Z., Shore, H. B. & Feher, G. (1978). *J. Mol. Biol.* **123**, 539–555.
Keller, A. (1968). *Rep. Prog. Phys.* **31**, 623–704.
Luft, J. R., Arakali, S. V., Kirisits, M. J., Kalenik, J., Wawrzak, I., Cody, V., Pangborn, W. A. & DeTitta, G. T. (1994). *J. Appl. Cryst.* **27**, 443–452.
Mackley, M. R. & Keller, A. (1975). *Philos. Trans. R. Soc. Lond.* **278**, 29–66.
Mackley, M. R., Wannaborworn, S., Gao, P. & Zhao, F. (1999). *Microsc. Anal.* **69**, 25–29.
Middaugh, C. R., Tisel, W. A., Haire, R. N. & Rosenberg, A. (1979). *J. Biol. Chem.* **254**, 367–370.
Miyashita, S., Komatsu, H., Suzuki, Y. & Nakada, T. (1994). *J. Cryst. Growth*, **141**, 419–424.
Penikova, A., Pan, W., Hodjaoglu, F. & Vekilov, P. G. (2006). *Ann. NY Acad. Sci.* **1077**, 214–231.
Rayleigh, Lord (1882). *Proc. Lond. Math. Soc.* **s1–14**, 170–177.
Rosenberger, F. (1986). *J. Cryst. Growth*, **76**, 618–636.
Shim, J.-U., Cristobal, G., Link, D. R., Thorsen, T. & Fraden, S. (2007). *Cryst. Growth Des.* **7**, 2192–2194.
Stevens, R. C. (2000). *Curr. Opin. Struct. Biol.* **10**, 558–563.
Tardieu, A., Bonneté, F., Finet, S. & Vivarès, D. (2002). *Acta Cryst.* D**58**, 1549–1553.
Taylor, G. (1950). *Proc. R. Soc. Lond. A Math. Phys. Sci.* **201**, 192–196.
Wiencek, J. M. (1999). *Annu. Rev. Biomed. Eng.* **1**, 505–534.